

RESEARCH PAPER

Topical delivery of bee venom through the skin by a water-in-oil nanoemulsion

Yaser Yousefpoor^{1,2}, Amir Amani^{3,4*}, Adeleh Divsalar⁵, Mohammad Reza Vafadar⁶

¹Department of Medical Nanotechnology, School of Advanced Technologies in Medicine, Tehran University of Medical Sciences, Tehran, Iran

²Research Center of Advanced Technologies in Medicine, Torbat Heydariyeh University of Medical Sciences, Torbat Heydariyeh, Iran

³Natural Products and Medicinal Plants Research Center, North Khorasan University of Medical Sciences, Bojnord, Iran

⁴Medical Biomaterials Research Center, Tehran University of Medical Sciences, Tehran, Iran

⁵Department of Cell & Molecular Biology, Faculty of Biological Sciences, Kharazmi University, Tehran, Iran

⁶Khalil Abad Health Center, Mashhad University of Medical Sciences, Mashhad, Iran

ABSTRACT

Objective(s): Bee venom (BV) contains peptides that do not pass through healthy skin due to their high molecular weight. Nanoemulsions (NEs) are capable of facilitating drug permeation through the skin.

Materials and Methods: We prepared water-in-oil (W/O) NEs containing BV with a mixture of Span 80, Tween 80, and olive oil by low energy method. Then, based on stability studies, four different NE formulations with 3, 5, 7, and 9% aqueous phase were chosen, each having different BV concentrations and characterized for their particle size, polydispersity index (PDI), viscosity, and refractive index. Afterwards, an NE preparation having 5% BV solution was used for skin permeation studies by Franz diffusion cell at three BV concentrations (i.e., 5000, 2500, and 1250 µg/ml).

Results: The results showed that by increasing the percentage of BV content (from 3 to 9 %) and surfactants (from 30 to 60 %), the size of NEs decreased while increasing BV concentration at a fixed percentage of BV content, led to increase in size and PDI. Skin permeation studies showed that after 12 h, NEs could permeate approximately 10 % of initial BV through the skin, depending on BV concentration in the NE.

Conclusion: The data showed that NEs could be used for topical delivery of peptides of BV through the skin

Keywords: Bee venom, Franz diffusion cell, Nano emulsion, Passing, Skin

How to cite this article

Yousefpoor Y, Amani A, Divsalar A, Vafadar MR. Developing a nanoemulsion for permeation of peptides of bee venom through the skin. *Nanomed J.* 2022;9(2):131-137. DOI: 10.22038/NMJ.2022.62398.1648

INTRODUCTION

Topical drug delivery can be beneficial to avoid problems such as first-pass metabolism and adverse effects of some drugs when taken orally [1, 2]. It has advantages compared with the parenteral route as the injection is associated with pain in the site of injection and hazardous medical wastes [3]. However, a main disadvantage of the topical route is low efficacy due to the presence of stratum corneum as a natural barrier for the permeation of many molecules. This necessitates using enhancers to disrupt the structure of the

stratum corneum to increase permeability [4]. In practice, many introduced penetration enhancers may be harmful and cause skin irritations, particularly in prolonged applications [5]. Also, they often fail to provide efficient permeation for many biologicals, especially those with high molecular weight or high water solubility properties [6]. Thus, it is desirable to develop alternative topical systems that do not use chemical penetration enhancers while facilitating drug permeation through the skin.

NEs are exciting options for this purpose [7]. Nanoemulsions (NEs) are homogeneous systems consisting of at least two immiscible liquids with a mean droplet diameter usually less than 100 nm. They exist in water-in-oil (W/O) or oil-in-water (O/W) forms (8-10). In order to prepare NEs,

* Corresponding author: Email: A.amani@nkums.ac.ir

Note. This manuscript was submitted on November 21, 2021; approved on January 24, 2022

surfactant(s) and an energy source are generally required [11]. NEs may be used as drug delivery systems with several advantages such as carrying both hydrophilic and hydrophobic components in a single formulation, improving bioavailability and drug loading, control of drug release, and protection from enzymatic degradation [12, 13]. Many studies have developed different formulations of NEs for topical delivery of hydrophilic compounds such as inulin [14], plasmid DNA [15], caffeine [16], and naproxen [17]. However, no work so far has used NEs for topical delivery of peptides/proteins.

Bee Venom (BV) is a bio-toxin composed of at least 18 active components, including enzymes, peptides, and biogenic amines, with a wide variety of pharmaceutical properties [18]. The main biologically active component of BV, Melittin, forms approximately 50% of the dry weight of BV. Melittin is a water-soluble, linear, cationic, hemolytic, cell lytic, and amphipathic peptide with a molecular weight of 2846.46 g/mol [19, 20]. It has several functions such as anti-inflammatory (in minimal doses), immunosuppressive, immune-stimulatory, anti-microbial, cytotoxicity (against cancer cells), anti-arthritic, and anti-atherosclerosis properties [21, 22]. BV therapy uses BV on specific skin points, which has treated some inflammatory diseases for ~3000 years [23]. The method is performed by live bee stings or injection of BV. However, both methods could cause pain, itching, or swelling [24]. Hence, we aimed to prepare a W/O NE formulation to deliver BV through the skin barriers. In this study, we investigated the permeation rate of BV through rat skin by Franz diffusion cell (FDC). This study aimed to introduce a painless method for topical/transdermal delivery of BV for medical applications.

MATERIALS AND METHODS

Materials

BV was obtained by electrical stimulation using the protocol suggested by Benton et al. [25]. It was collected from healthy hives, *Apis mellifera medaparsica* strain, from northeast areas of Iran. Sorbitan monooleate (Span 80) and poly-oxyethylene 20 sorbitan monooleate (Tween 80) as surfactants were purchased from Merck Chemicals (Germany). Olive oil was from Fadak Co. (Iran), and bichinchonic acid (BCA) was from Biotech Co. (Iran).

Animals

Male Wistar rats, weighing ~ 250 g, were used in this study, were kept according to the standard laboratory animal guidelines. The ethics

committee of tehran university of medical sciences approved the experimental protocols (IR.TUMS.VCR.REC.1396.4285).

Methods

Preparation of NEs

To prepare W/O NE, a stock solution of BV in deionized water was prepared and diluted to obtain serial dilutions of BV (i.e., 5000, 2500, 1250, 625, 312, 156, and 0 µg/ml) as aqueous phase (aq). Then, surfactants (Smix: Span 80 and Tween 80) were added to the solutions and mixed using a magnetic stirrer (MS-300HS, Protraction Intertrade Co., Korea) (1000 rpm, 5 min, room temperature). Eventually, olive oil as the oil phase was added and mixed thoroughly (1000 rpm, 5 min, room temperature).

Physical stability of NEs

NEs were centrifuged (3500 rpm, 30 min, 25 °C) to estimate the physical stability. Also, they were subjected to thermal stress analyses (three heating-cooling cycles between 4 and 45 °C and three freeze-thaw cycles between -20 and 25 °C with storage at each temperature for 12 h). After each cycle, samples were examined by macroscopic observation for signs of phase separation [26, 27]. The results of the stability studies were used to shape the pseudo-ternary phase diagram.

Viscosity and refractive index

The viscosity of NEs was measured by a modular compact rheometer (Physica-MCR300, Anton Paar GmbH, Austria) at 25 °C. The shear stress was measured as a function of the shear rate from 0.1 to 100 s⁻¹.

The refractive index of NEs was measured using an Abbe refractometer (Bausch and Lomb Optical, USA) by examining one drop of the NEs at 25 °C.

DLS studies

The mean droplet size of NEs was measured by dynamic light scattering (DLS) at a scattering angle of 90° at 25 °C using a Scatterscope I (K-ONE Ltd. Korea). The polydispersity index (PDI) was used for the assessment of the size distribution of NEs. It assumed a single size population following a Gaussian distribution and was analyzed as the square of the ratio of the standard deviation to mean droplet size, which indicates the uniformity of droplet size [28]. The size and stability studies were employed to determine the optimum NE preparation for further studies.

Ex vivo skin permeation studies

Skin permeation studies were performed by an FDC with an effective diffusional area of 4.9 cm², having a donor chamber filled with 10 ml NE, and a receiver chamber filled with 35 ml normal saline solution (NS) pH~7.4. Shaved abdominal skins of the rats were excised with the thickness (0.2-0.5 mm). The subcutaneous tissue was removed surgically, and the dermis side was wiped with isopropyl alcohol to remove adhering fats. The skins were mounted between the donor and receiver chambers of the FDC so that the stratum corneum side faced the former and the dermal side faced the latter. Skins were visually examined for possible physical damage before the experiments [2, 29]. The temperature of FDCs was fixed at 37 ± 0.5 °C by water circulation. The chambers of FDCs were placed on a stirrer (MS-300HS, Protraction Intertrade Co., Korea), and a magnetic stirrer (100 rpm) in receptor solution was continuously stirred during the experiment.

For the permeation studies, NE samples having 5% aq phase at three different BV solutions (5000, 2500, and 1250 µg/ml) and 40% Smix were employed. Sampling times were 0, 2, 4, 6, 8, 10, and 12 h, and the peptide concentration was determined using the BCA method. A blank group containing NE without BV was used to eliminate the effect of skin proteins in BCA results. The experiments were conducted in triplicate.

Permeation data analysis

The following equations were employed to calculate *Corrected BV Concentration* (C'n, due to dilution error of NS replenishment) in equation (1), *Permeation Rate* (Q, as the cumulative amount of permeated BV through the skin), *Steady-State Flux* (Jss, as the slope of the linear portion of the curve of the cumulative amount of BV per unit area versus time (h)), *Permeability Coefficient* (Kp, assuming sink conditions) in equation (2), *Diffusion Coefficient* (D) and *Skin Permeation Percentage at 12 h* (SPP12h) in equations (3, and 4), respectively [2, 30, 31]:

Equation (1): $C'n = Cn (Vt / Vt - Vs) (C'n^{-1} / Cn^{-1})$

C'n: corrected BV concentration of sample No. n, Cn: BV concentration of sample No. n, C'n⁻¹: corrected BV concentration of sample No. n⁻¹, Cn⁻¹: measured BV concentration of sample No. n⁻¹, Vt: total volume of receiver chamber capacity, Vs: volume of the sample

Equation (2): $Kp = Jss / BVO$

BVO: initial value of BV in the donor chamber (µg)

Equation (3): $D = Kp \times A^2$

A: effective absorption area

Equation (4): $SPP12h = (BV12h / BVO) \times 100$

BV12h: the total amount of permeated BV through the skin in the receiver chamber at 12 h (µg)

Statistical analysis

One-way analysis of variance and post-hoc Tukey tests were performed to assess the statistical significance of differences. Results with a P-value < 0.05 were considered statistically significant. Statistical analyses were carried out using the SPSS software, v. 19 (SPSS, Inc., USA).

RESULTS

Preparation of NEs

Stable NEs were created at HLB 10 with aq 3, 5, 7, and 9% aq phase (BV: 0 µg/ml). Fig. 1 shows pseudo-ternary phase diagrams for the stable NEs as the black region and unstable NEs as the gray region at different ingredients' concentrations.

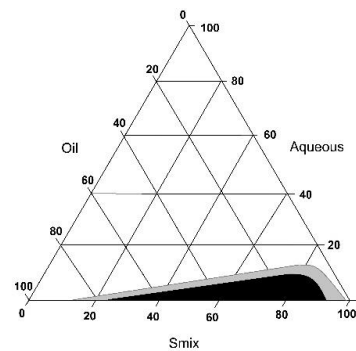


Fig. 1. Pseudo-ternary phase diagram indicating stable W/O nanoemulsion (black region) and unstable nanoemulsion (gray region)

Table 1. Formulation, viscosity and refractive index of 4 stable nanoemulsions

Samples	% aq content	%Smix	%Span 80	%Tween 80	%Olive Oil	Viscosity (cP)	Refractive index
NE1	3	30	14	16	67	174±3	1.465
NE2	5	40	18.7	21.3	55	243±7	1.466
NE3	7	50	23.4	26.6	43	362±8	1.468
NE4	9	60	28	32	31	409±21	1.470

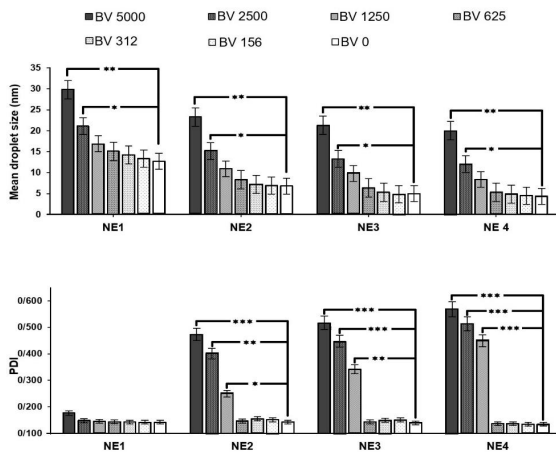


Fig. 2. Top: Mean \pm SE droplet size (nm), bottom: polydispersity index (PDI) \pm SE of four nanoemulsion samples having seven different concentrations of BV in their internal phase (5000, 2500, 1250, 625, 312, 156, and 0 $\mu\text{g/ml}$)

Characterization of NEs

Table 1 shows the viscosity (cP) and refractive index of the most stable NEs. With increasing, the Smix content (i.e., NE1 to NE4), the viscosity increased from 174 to 409 cP. The refractive index also indicated a minimal increase from 1.465 to 1.470.

Fig. 2 shows the mean droplet size and PDI of 4 NEs having seven different concentrations of BV (0 to 5000 $\mu\text{g/ml}$) in their internal phase. The data shows that by increasing the aq phase and Smix contents (i.e., NE1 to NE4), the particle size decreased slightly, but PDI showed an increase. While by increasing BV concentration from 0 to 5000 $\mu\text{g/ml}$, particle size and PDI increased.

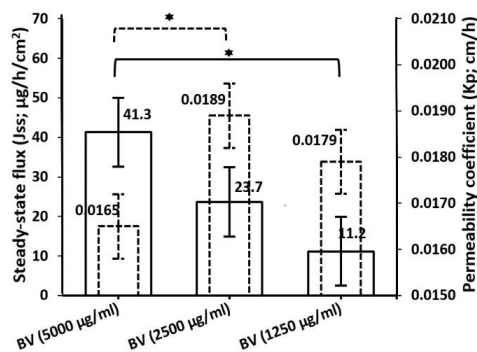


Fig. 4. Steady-state flux (J_{ss} , continuous borderline) and permeability coefficient (K_p , dashed borderline) of NE2 containing three BV concentrations in their internal phase (5000, 2500, and 1250 $\mu\text{g/ml}$). * shows P -value $<$ 0.05

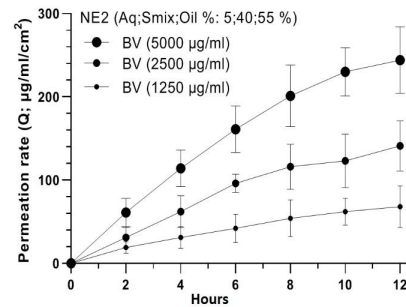


Fig. 3. Permeation rate (Q ; $\mu\text{g/ml/cm}^2$) of 10 ml NE2 containing three BV concentrations in their internal phase (5000, 2500 and 1250 $\mu\text{g/ml}$)

Ex vivo skin permeation studies

The skin permeation studies were performed on NE2, and the results are given in Figs 3-5. Fig. 3 shows that the permeation rate (Q) increased during the study period. Furthermore, higher BV contents showed higher Q values.

Fig. 4 shows steady-state flux (J_{ss}) and permeability coefficient (K_p) for the NE2 containing three different BV concentrations at its internal phase (i.e., 5000, 2500, and 1250 $\mu\text{g/ml}$). In comparison, J_{ss} tends to decrease significantly ($P < 0.05$) by decreasing BV content from 41.3 $\mu\text{g/h/cm}^2$ (for BV concentration of 5000 $\mu\text{g/ml}$ in the internal phase) to 11.2 $\mu\text{g/h/cm}^2$ (for BV concentration of 1250 $\mu\text{g/ml}$ in the internal phase). Furthermore, there was no apparent pattern for changes in K_p as a function of BV concentration.

Fig. 5 shows the diffusion coefficient (D) and skin permeation percentage at 12 h (SPP12h) for NE2 containing three considered BV concentrations.

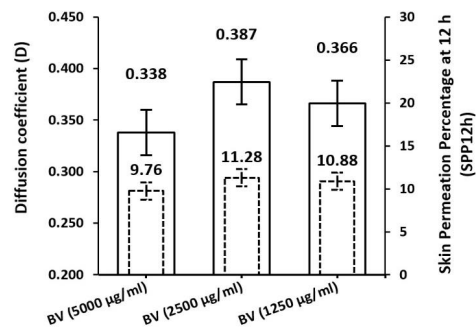


Fig. 5. Diffusion coefficient (D , continuous borderline) and skin permeation percentage (SPP12h, dashed borderline) of NE2 containing three BV concentrations in their internal phase (5000, 2500, and 1250 $\mu\text{g/ml}$)

From the details, at 5000, 2500, and 1250 $\mu\text{g}/\text{ml}$ BV concentrations mean of SPP12h was 9.76, 11.28, and 10.88% of initial BV, and mean of D was 0.338, 0.387, and 0.366, respectively. The findings show there was no significant change for SPP12h and D as a function of BV concentration.

DISCUSSION

The results of this study indicated that NEs could deliver BV as a hydrophilic peptide through the skin. Several studies so far have reported the permeation of different molecules by NEs [29, 31-33]. However, minimal studies have focused on the preparation of NEs containing peptides/proteins. To ensure diffusion across the stratum corneum, molecular weight less than 500 Daltons is assumed to be essential [34], while peptides/proteins are typically larger than this cut-off value [35]. Accepting a limitation of our study, which was the possible effects of nanoemulsion ingredients on the molecular structure of BV, we managed to show that NEs could pass BV through rat skin layers. More works on the effect of independent parameters such as concentration and size are essential before making a final judgment on the efficacy of NEs in topical/transdermal delivery of peptides/proteins. For instance, the effect of concentration of the drug as a driving force for the percutaneous absorption of the drug [36] needs to be investigated in more detail.

During the process of preparation of NEs, the primary indicator for the formation of NEs is the formation of a monophasic and transparent dispersion to be visually confirmed. We performed stability studies to evaluate any signs of sedimentation, creaming, or phase separation [37]. Sedimentation/creaming usually occurs when external forces (e.g., earth gravity) overcome the Brownian motion of the droplets [38]. The HLB value should be optimized to achieve the maximum stability of NEs. The optimum HLB value obtained in this study was 10. In a previous report, for stabilization of a nanoemulsion containing octane as oil phase and Span 80/Tween 80 as surfactants, an HLB value of 9 was employed [39]. Reviewing the literature, W/O NEs with 5% [40] and 2.7% [14] water have been reported using Span 80 and Tween 80 as surfactants, similar to our findings.

Our data showed that by increasing aq phase and surfactant concentrations, the viscosity increased, probably due to the effect of surfactant. However, the refractive index did not change

considerably, similar to a previous work in which the refractive index varied from 1.401 to 1.411 when Smix increased from 2:1 to 4:1 [29]. The refractive indices of Span 80, Sween 80, and olive oil are 1.480, 1.473, and 1.460, respectively [41-44]. Therefore, changes in their contents are not expected to change the refractive index of the preparation.

Assessment of mean droplet size for the selected NEs stated that particle size increased when BV concentration increased in a fixed aq phase percentage. The effect of the internal phase on the particle size of nanoemulsions has been reported previously [45]. Additionally, we found that size had been decreased by increasing the amount of surfactants, as reported previously [46], which can happen due to the increase of surfactant molecules which cause more stable NEs to form smaller droplets [47].

Our findings showed that by increasing BV concentration, permeation rate and steady-state flux increased. While other parameters, including permeability coefficient, diffusion coefficient, and skin permeation percentage at 12 h, did not change significantly as a function of BV concentration. Harwansh et al. [33] studied the transdermal delivery of glycyrrhizin by NEs and showed that the permeation rate of NEs increased linearly as a function of the loading dose, under Fick's first law of diffusion. They also reported that the permeation rate of NEs followed zero-order release kinetics.

A second mechanism that may affect the permeation rate is particle size. Previously, a direct correlation between permeation rate and size of NEs containing fluvastatin has been reported when the particle size decreased from 128.8 nm to 88.4 nm (i.e., from 54.4 to 78.8 $\mu\text{g}/\text{ml}/\text{cm}^2$) [48]. However, a decrease in the particle size to 66.9 nm and 11.7 nm did not change the permeation rate anymore [48]. Apparently, below a cut-off value, size is not affecting the permeation rate anymore. As the particle size of our NE was below 23.3 nm, our findings appear to agree well with the study as mentioned above.

CONCLUSION

Our study showed that BV peptides could be carried using W/O NEs. The W/O NE managed to pass BV through the skin, depending on BV content. Approximately 10 % of initial BV permeated through the skin after 12 h. This novel delivery

system may be introduced as an alternative to injections with advantages such as painless and improved patient compliance.

ACKNOWLEDGMENTS

We would like to extend our sincere thanks to those who collaborated. This project was supported by the Tehran University of Medical Sciences (Grant No. 96-04-87-37262).

COMPETING INTERESTS

All authors declare no conflict of interest.

REFERENCES

1. Wiechers JW. The barrier function of the skin in relation to percutaneous absorption of drugs. *Pharm Weekbl Sci*. 1989;11(6):185-198.
2. Bartosova L, Bajgar J. Transdermal drug delivery *in vitro* using diffusion cells. *Curr Med Chem*. 2012;19(27):4671-4677.
3. Prausnitz MR, Langer R. Transdermal drug delivery. *Nat Biotechnol*. 2008;26(11):1261.
4. López A, Llinares F, Cortell C, Herraiz M. Comparative enhancer effects of Span® 20 with Tween® 20 and Azone® on the *in vitro* percutaneous penetration of compounds with different lipophilicities. *Int J Pharm*. 2000;202(1-2):133-140.
5. Yousefpoor Y, Bolouri B, Bayati M, Shakeri A, Eskandari Y. The combined effects of Aloe vera gel and silver nanoparticles on wound healing in rats. *Nanomed J*. 2016;3(1):57-64.
6. Lipinski CA, Lombardo F, Dominy BW, Feeney PJ. Experimental and computational approaches to estimate solubility and permeability in drug discovery and development settings. *Adv Drug Deliv Rev*. 1997;23(1-3):3-25.
7. Abbasifard M, Yousefpoor Y, Amani A, Arababadi MK. Topical Bee Venom Nano-emulsion Ameliorates Serum Level of Endothelin-1 in Collagen-Induced Rheumatoid Arthritis Model. *Bionanoscience*. 2021.
8. Junqueira LA, Amaral TN, Leite Oliveira N, Prado MET, de Resende JV. Rheological behavior and stability of emulsions obtained from *Pereskia aculeata* Miller via different drying methods. *Int J Food Prop*. 2018;21(1):21-35.
9. Chime S, Kenechukwu F, Attama A. Nanoemulsions—advances in formulation, characterization and applications in drug delivery: chapter; 2014.
10. Osanloo M, Amani A, Sereshti H, Abai MR, Esmaili F, Sedaghat MM. Preparation and optimization nanoemulsion of Tarragon (*Artemisia dracuncululus*) essential oil as effective herbal larvicide against *Anopheles stephensi*. *Ind Crops Prod*. 2017;109:214-219.
11. Eid AM, Baie SH, Arafat O, editors. Development and stability evaluation of olive oil nanoemulsion using sucrose monoester laurate. *AIP Conf Proc*; 2012: AIP.
12. Kotta S, Khan AW, Pramod K, Ansari SH, Sharma RK, Ali J. Exploring oral nanoemulsions for bioavailability enhancement of poorly water-soluble drugs. *Expert Opin Drug Deliv*. 2012;9(5):585-598.
13. Azizi M, Esmaili F, Partoazar A, Ejtemaei Mehr S, Amani A. Efficacy of nano-and microemulsion-based topical gels in delivery of ibuprofen: an *in vivo* study. *J Microencapsul*. 2017;34(2):195-202.
14. Wu H, Ramachandran C, Weiner ND, Roessler BJ. Topical transport of hydrophilic compounds using water-in-oil nanoemulsions. *Int J Pharm*. 2001;220(1-2):63-75.
15. Wu H, Ramachandran C, Bielinska AU, Kingzett K, Sun R, Weiner ND, et al. Topical transfection using plasmid DNA in a water-in-oil nanoemulsion. *Int J Pharm*. 2001;221(1-2):23-34.
16. Shakeel F, Ramadan W. Transdermal delivery of anticancer drug caffeine from water-in-oil nanoemulsions. *Colloids Surf B Biointerfaces*. 2010;75(1):356-362.
17. Abd E, Namjoshi S, Mohammed YH, Roberts MS, Grice JE. Synergistic skin penetration enhancer and nanoemulsion formulations promote the human epidermal permeation of caffeine and naproxen. *J Pharm Sci*. 2016;105(1):212-220.
18. Yousefpoor Y, Amani A, Divsalar A, Mousavi SE, Torbaghan YE, Emami O. Assessment of hemolytic activity of bee venom against some physicochemical factors. *J Asia Pac Entomol*. 2019;22(4):1129-1135.
19. Mahmoodzadeh A, Morady A, Zarrinnahad H, Bagheri KP, Ghasemi-Dehkordi P, Mahdavi M, et al. Isolating Melittin from Bee Venom and Evaluating its Effect on Proliferation of Gastric Cancer Cells. *Basic & Clinical Cancer Research*. 2013;5(4):26-32.
20. Fidelio GD, Maggio B, Cumar FA. Interaction of myelin basic protein, melittin and bovine serum albumin with gangliosides, sulphatide and neutral glycosphingolipids in mixed monolayers. *Chem Phys Lipids*. 1984;35(3):231-245.
21. Son DJ, Lee JW, Lee YH, Song HS, Lee CK, Hong JT. Therapeutic application of anti-arthritis, pain-releasing, and anti-cancer effects of bee venom and its constituent compounds. *Pharmacol Ther*. 2007;115(2):246-270.
22. Oršolić N. Bee venom in cancer therapy. *Cancer Metastasis Rev*. 2012;31(1-2):173-194.
23. Zhang S, Liu Y, Ye Y, Wang X-R, Lin L-T, Xiao L-Y, et al. Bee venom therapy: Potential mechanisms and therapeutic applications. *Toxicon*. 2018;148:64-73.
24. Ali M. Studies on bee venom and its medical uses. *Int J Adv Res Technol*. 2012;1(2):69-83.
25. Benton AW, Morse RA, Stewart JD. Venom collection from honey bees. *Science*. 1963;142(3589):228-230.
26. Azeem A, Rizwan M, Ahmad FJ, Iqbal Z, Khar RK, Aqil M, et al. Nanoemulsion components screening and selection: a technical note. *AAPS PharmSciTech*. 2009;10(1):69-76.
27. Najafi-Taher R, Ghaemi B, Amani A. Delivery of adapalene using a novel topical gel based on tea tree oil nanoemulsion: Permeation, antibacterial and safety assessments. *Eur J Pharm Sci*. 2018;120:142-151.
28. Arzenšek D, Podgornik R, Kuzman D, editors. Dynamic light scattering and application to proteins in solutions. Seminar, Department of Physics, University of Ljubljana; 2010.
29. Shakeel F, Baboota S, Ahuja A, Ali J, Aqil M, Shafiq S. Nanoemulsions as vehicles for transdermal delivery of aceclofenac. *AAPS PharmSciTech*. 2007;8(4):191.
30. Akhtar N, Rehman M, Khan H, Rasool F, Saeed T, Murtaz G. Penetration enhancing effect of polysorbate 20 and 80 on the *in vitro* percutaneous absorption of l-ascorbic acid. *Trop J Pharm Res*. 2011;10(3).
31. Alkilani AZ, Hamed R, Al-Marabeh S, Kamal A, Abu-Huwajj R, Hamad I. Nanoemulsion-based film formulation for transdermal delivery of carvedilol. *J Drug Deliv Sci Technol*. 2018;46:122-128.
32. Khurana S, Jain N, Bedi P. Nanoemulsion based gel for transdermal delivery of meloxicam: physico-chemical, mechanistic investigation. *Life sciences*. 2013;92(6-7):383-392.
33. Harwansh RK, Patra KC, Pareta SK, Singh J, Rahman MA.

- Nanoemulsions as vehicles for transdermal delivery of glycyrrhizin. *Braz J Pharm Sci* 2011;47(4):769-778.
34. Brown MB, Martin GP, Jones SA, Akomeah FK. Dermal and Transdermal Drug Delivery Systems: Current and Future Prospects. *Drug Delivery*. 2006;13(3):175-187.
 35. Abbasi-Ghahramanloo A, Safiri S, Gholami A, Yousefpoor Y, Babazadeh S, Torkamannejad Sabzevari J. Spatio-temporal epidemiologic mapping, modeling and prediction of tuberculosis incidence rate in northeast of Iran. *J Anal Res Clin Med*. 2017;5(3):103-109.
 36. Prausnitz MR, Elias PM, Franz TJ, Schmuth M, Tsai J-C, Menon GK, et al. Skin barrier and transdermal drug delivery. *Dermatology*. 2012;3:2065-2073.
 37. Valizadeh A, Shirzad M, Pourmand MR, Farahmandfar M, Sereshti H, Amani A. Levofloxacin nanoemulsion gel has a powerful healing effect on infected wound in streptozotocin-induced diabetic rats. *Drug Deliv Transl Res*. 2021;11(1):292-304.
 38. Tadros TF. Emulsion formation, stability, and rheology. *Emulsion formation and stability*. 2013;1:1-75.
 39. Fu Z, Liu M, Xu J, Wang Q, Fan Z. Stabilization of water-in-octane nanoemulsion. Part I: Stabilized by mixed surfactant systems. *Fuel*. 2010;89(10):2838-2843.
 40. Porras M, Solans C, González C, Martínez A, Guinart A, Gutiérrez JM. Studies of formation of W/O nano-emulsions. *Colloids Surf A Physicochem Eng Asp*. 2004;249(1-3):115-8.
 41. Shakeel F, Baboota S, Ahuja A, Ali J, Faisal M, Shafiq S. Stability evaluation of celecoxib nanoemulsion containing Tween 80. *Thai J Pharm Sci*. 2008;32:4-9.
 42. Kassem MG, Ahmed A-MM, Abdel-Rahman HH, Moustafa AH. Use of Span 80 and Tween 80 for blending gasoline and alcohol in spark ignition engines. *Energy Reports*. 2019;5:221-230.
 43. Sinzato YZ, Dias NJS, Cunha FR. An experimental investigation of the interfacial tension between liquid-liquid mixtures in the presence of surfactants. *Exp Therm Fluid Sci*. 2017;85:370-378.
 44. Jaffar AF, Akram IN, Salman AM, Al-Taai QA. Nonlinear properties of olive oil films doped with poly (methyl methacrylate), polystyrene and their blend by using z-scan technique. *International Journal*. 2020.
 45. Alvarado H, Abrego G, Souto E, Garduño-Ramirez M, Clares B, García M, et al. Nanoemulsions for dermal controlled release of oleanolic and ursolic acids: *in vitro*, *ex vivo* and *in vivo* characterization. *Colloids Surf B Biointerfaces*. 2015;130:40-47.
 46. Khani S, Abbasi S, Keyhanfar F, Amani A. Use of artificial neural networks for analysis of the factors affecting particle size in mebudipine nanoemulsion. *J Biomol Struct Dyn*. 2019;37(12):3162-3167.
 47. Kumar A, Kushwaha V, Sharma PK. Pharmaceutical microemulsion: Formulation, characterization and drug deliveries across skin. *Int J Drug Dev Res*. 2014;6(1):1-21.
 48. Kaur R, Ajitha M. Transdermal delivery of fluvastatin loaded nanoemulsion gel: Preparation, characterization and *in vivo* anti-osteoporosis activity. *Eur J Pharm Sci*. 2019;136:104956.